Numerical Solutions for Swinging Atwood's Machine

Étienne Cadotte, Irina Nitu

December 5, 2023

1 Introduction

In 1784, English mathematician George Atwood implemented an experiment to verify the laws of motion. It consisted of two masses connected by a mass-less string passing over a pulley, with each mass dangling on one side of the pulley. Under the influence of gravitational acceleration, the heavier mass slides down, pulling the smaller mass up along the vertical axis[1]. While such a problem is quite simple to analyse and is often used in high school, it's simplicity is based on an assumption that the motion of the masses are locked about the vertical axis, thus neglecting the angular motion of the masses. In this paper, we will analyse the much more complex problem involving one or both masses free to rotate. We will make use of explicit integrators to numerically resolve the mass trajectories for various sets of values and analyze the numerical precision of our simulations, namely with respect to conservation of energy.[...] TODO

2 The Equations of Motion

Before doing any numerical work on the system, we need to find the equation of motions of the system. Here, we will derive them through Hamiltonian dynamics. Assuming a mass-less string and small pulley, we can write the kinetic energy as :

$$T = \frac{1}{2}M\dot{r}^2 + \frac{1}{2} * m * (\dot{r}^2 + r^2\dot{\theta}^2),$$

which comes from $T = \frac{1}{2}mv^2 + \frac{1}{2}I\omega^2$. We are assuming that the mass M is the larger one and mass m is the only mass which is swinging.

Since the only potential field in the problem is gravitational, we can define the potential energy with zero point $r = 0$ thus leading to

$$U = -Mg(R - r) - mgr\cos\theta$$
$$U = -MgR + Mgr - mgr\cos\theta,$$

Where R is the total length of the rope. Since $-MgR$ is a constant in the potential, we can remove it without any impact on the dynamics of the system, which gives us the following equation:

$$U = Mgr - mgr\cos\theta.$$

This leaves us with the Lagrangian :

$$L = T - U = \frac{1}{2}M\dot{r}^2 + \frac{1}{2} * m * (\dot{r}^2 + r^2\dot{\theta}^2) - Mgr + mgr\cos\theta,$$

[1] [INSERT REFERENCE]

which means:

$$p_r = \frac{\partial L}{\partial \dot{r}} = (M+m)\dot{r} \quad \text{and} \quad p_\theta = \frac{\partial L}{\partial \dot{\theta}} = mr^2\dot{\theta}$$

$$\dot{r} = \frac{p_r}{M+m} \quad \text{and} \quad \dot{\theta} = \frac{p_\theta}{mr^2}.$$

We are now able to formulate the Hamiltonian as :

$$H = T + U$$

$$H = \frac{p_r^2}{2(M+m)} + \frac{p_\theta^2}{2mr^2} + Mgr - mgr\cos\theta \tag{1}$$

Which we then use to find the derivatives of momentum:

$$\dot{p_r} = -\frac{\partial H}{\partial r} = \frac{p_\theta^2}{mr^3} - Mg + mg\cos\theta \quad \text{and} \quad \dot{p_\theta} = -\frac{\partial H}{\partial \theta} = -mgr\sin\theta.$$

We then obtain the following equations of motion:

$$\begin{cases} \dot{r} = \frac{p_r}{M+m} \\ \dot{\theta} = \frac{p_\theta}{mr^2} \\ \dot{p_r} = \frac{p_\theta^2}{mr^3} - Mg + mg\cos\theta \\ \dot{p_\theta} = -mgr\sin\theta \end{cases} \tag{2}$$

which matches with the equation of motion from the literature[2].

While these derivations consider the case of a single swinging mass, we will also use results from the two swinging mass case which resolves to the following Hamiltonian:

$$H = \frac{p_r^2}{2(M+m)} + \frac{p_{\theta_M}^2}{2M(R-r)^2} + \frac{p_{\theta_m}^2}{2mr^2} - Mg(R-r)\cos\theta_M - mgr\cos\theta_m, \tag{3}$$

with corresponding equations of motion:

$$\begin{cases} \dot{r} = \frac{p_r}{M+m} \\ \dot{\theta}_M = \frac{p_{\theta_M}}{M(R-r)^2} \\ \dot{\theta}_m = \frac{p_{\theta_m}}{mr^2} \\ \dot{p_r} = -\frac{p_{\theta_M}^2}{M(R-r)^3} + \frac{p_{\theta_m}^2}{mr^3} - Mg\cos\theta_M + mg\cos\theta_m \\ \dot{p}_{\theta_M} = -Mg(R-r)\sin\theta_M \\ \dot{p}_{\theta_m} = -mgr\sin\theta_m \end{cases} \tag{4}$$

The equations of motion we have just derived above for the single swinging mass (eq. 2), as well as for system with two swinging masses (eq. 4) will serve as our basis in our numerical resolution of mass motion.

[2]Nick Tufillaro; Integrable motion of a swinging Atwood's machine. Am. J. Phys. 1 February 1986; 54 (2): 142–143. https://doi.org/10.1119/1.14710

3 Independence Under Mass Multiplication

The first thing to be noted, as it will impact the rest of this paper, is that the dynamics of the system do not change for different masses corresponding to the same mass ratio μ; as we can see from Figure 1, the motion stays the same. With numerical analysis we find they are similar in numerical precision, thus proving that the system is only dependent on mass ratio μ, which can also be shown analytically. The method used to produce this figure will be explained in the next section. We can thus set mass $m = 1$ without any loss of generality. This lets us simplify the Hamiltonian (1) and the equations of motion(2) for the system with one swinging mass to the following:

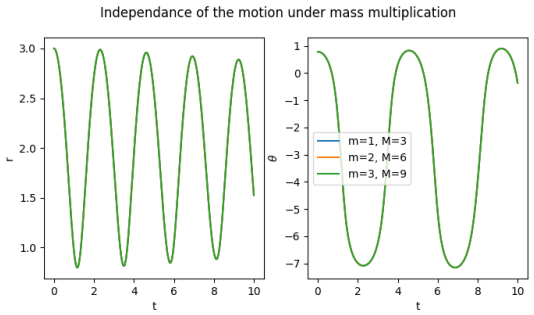

Figure 1: Paths for different masses with same mass ratio μ. The curves for the evolution of coordinates r and θ in time are the same for different masses that resolve to the same mass ratio μ.

$$H = \frac{p_r^2}{2(\mu+1)} + \frac{p_\theta^2}{2r^2} + \mu g r - g r \cos\theta \tag{5}$$

$$\begin{cases} \dot{r} = \frac{p_r}{\mu+1} \\ \dot{\theta} = \frac{p_\theta}{r^2} \\ \dot{p_r} = \frac{p_\theta^2}{r^3} - \mu g + g\cos\theta \\ \dot{p_\theta} = -gr\sin\theta \end{cases} \tag{6}$$

4 Our Integrators

Numerical solutions to the swinging atwood's machine were implemented with the use of an RK4 integrator which involves computing the coordinates of the system in time with four steps. We generalize the equations of motion from 2 to the following form:

$$\frac{dy(t)}{dt} = f(y(t), t). \tag{7}$$

The steps involved in the RK4 update are then

$$\begin{aligned} k_1 &= f(t_0, y(t_0)) \\ k_2 &= f(t_0 + \frac{\Delta t}{2}, y(t_0) + k_1\frac{\Delta t}{2}) \\ k_3 &= f(y(t_0) + k_2\frac{\Delta t}{2}, t_0 + \frac{\Delta t}{2}) \\ k_4 &= f(y(t_0) + k_3\Delta t, t_0 + \Delta t), \end{aligned}$$

for each canonical coordinate r, θ, p_r and p_θ, which gives us the following implementation:

```
import numpy as np

def RK4(nsteps, dt, x0, derivs):
    x = np.zeros((nsteps, len(x0)))
    x[0] = x0
    break_i = nsteps
    for i in range(1,nsteps):
```

```
        f = derivs((i-1)*dt, x[i-1])
        f1 = derivs((i-1)*dt + dt/2, x[i-1] + f*dt/2)
        f2 = derivs((i-1)*dt + dt/2, x[i-1] + f1*dt/2)
        f3 = derivs(i*dt, x[i-1] + f2*dt)
        x[i] = x[i-1] + dt*(f + 2*f1 + 2*f2 + f3)/6

        if x[i][0] <= 0.1 :
            break_i = i
            break

    return x, break_i
```

where x is the vector containing the canonical coordinates r, θ, p_r, p_θ of the SAM system, and the *derivs* parameter corresponds to a function implementing equations 2 as follows:

```
import numpy as np
import scipy.constants

def derivs(t,x):
    r,pr,theta,p_theta = x
    dr = pr/(M+m)
    dpr = p_theta**2 / (m*r**3) - M*scipy.constants.g + m*scipy.constants.g*np.cos(theta)
    dtheta = p_theta / (m*r**2)
    dp_theta = -m*scipy.constants.g*r*np.sin(theta)
    return np.array([dr,dpr,dtheta,dp_theta])
```

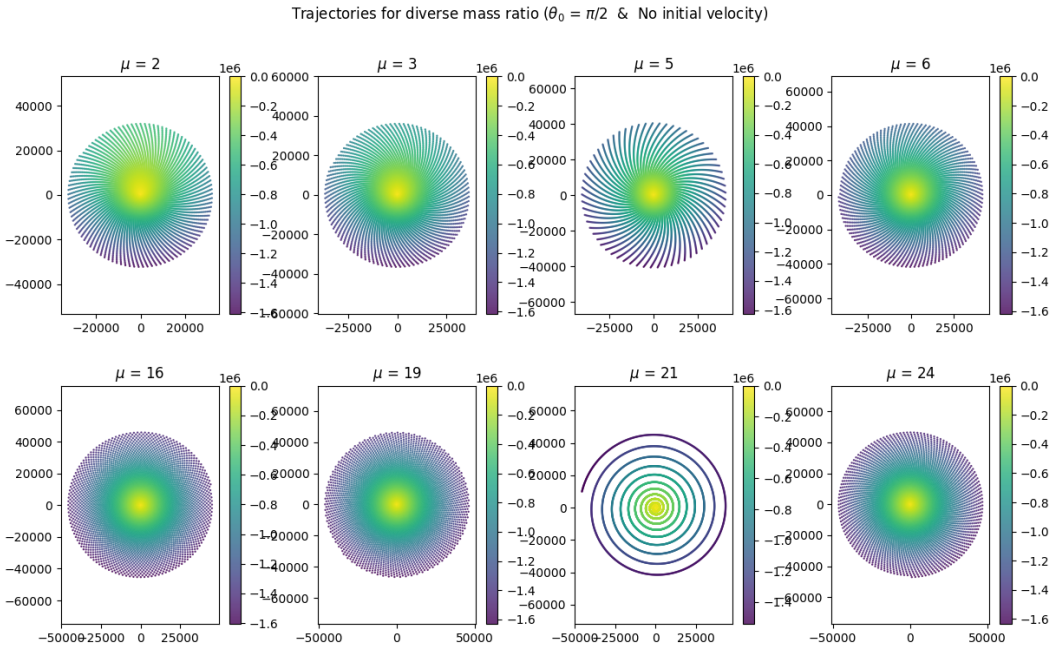

Figure 2: Euler-Cromer integration of the swinging atwood's machine's smaller mass.

An attempt at resolving the trajectories of the masses was made with the use of a Euler-Cromer integrator which makes use of second derivatives to update the coordinates of the system in time according to:

$$\dot{x}_{n+1} = \dot{x}_n + \ddot{x}_n \Delta t$$
$$x_{n+1} = x_n = \dot{x}_{n+1} \Delta t,$$

where x corresponds to the canonical coordinates of the system. We were unable to resolve the trajectories of the masses, which are illustrated in figure 2.

In the repository we can find an animated simulation of the system for mass ratio $\mu = 3$ ($results/Anim\_u = 3 - 1S - Explicit.gif$). On the right hand side of the animation we show the difference from the initial energy as a percentage. As we can see, the energy is properly conserved, which is expected for the Hamiltonian of a closed system. The reason why this value of mass ratio μ has been chosen is because it is the only properly integrable case of this system as shown by Nick Tufillaro [3]. Please note that while this is the only properly integrable case, we will not restrict ourselves to it in this paper as we are using numerical simulations.

Please also note how the trajectory followed in the animation is non-singular and quasiperiodic; in this paper we will limit our classification to singular or not singular, and periodic, quasiperiodic or chaotic. The fact that the path in the current simulation is only quasi-periodic means that the if we did use a symplectic integrator, the improvement in the conservation of the Hamiltonian would have only been marginal as these integrators are specifically used for periodic motions.

As already stated, a good measurement of the quality of our integrator is the conservation of energy. Different integrators will follow different lines on a logarithmic plot of the change in energy dE at the final time by the number of step to reach said time. To do such an analysis we use our integrator and iterate over an array of step size and save the energy error at the final time for each step size.

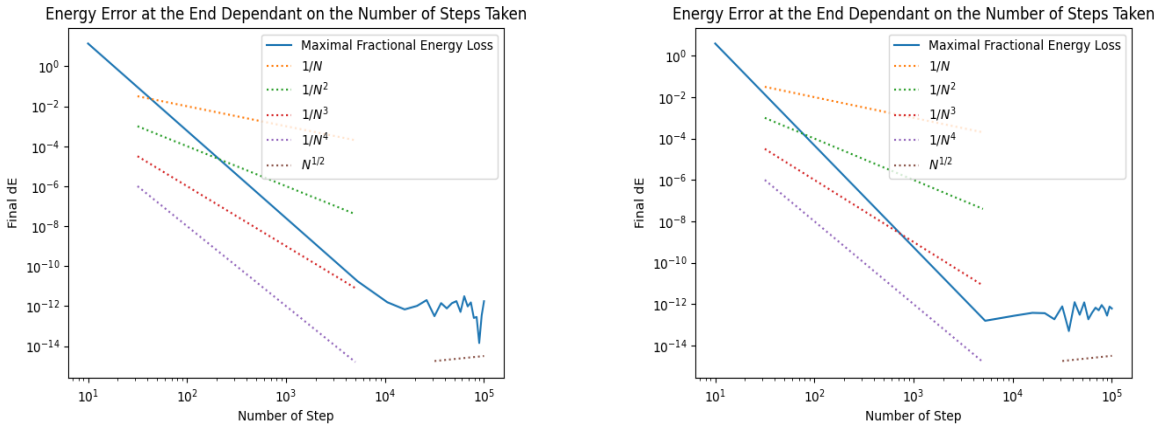

(a) Energy Error as a Function of Step Number for Quasiperiodic Motion (μ=3)

(b) Energy Error by Number of Step for Periodic Motion With P=pi (μ=1.665)

Figure 3: Energy Errors by Step Number for the 1 Swinging System

This produces Figure 3a. As we can see, the base error is very large since this is a complex system but seems to follow the $1/N^4$ slope which is similar to the performance of leapfrog[4] in that regard. Overall, the number of step required to reach what is the round off limit of $N^{1/2}$ given by Brouwer's Law[5] is about 10^5 which is once again comparable to leapfrog.

But, as stated previously, the motion for $\mu = 3$ is only quasiperiodic. And while symplectic integrators do especially better over full periodic orbit, explicit integrators such as our own do also get some benefit. For a swinging Atwood machine, it is known from literature that a mass ratio $\mu = 2.394$ results in a periodic path [6]. This can be visually confirmed through the animation for $\mu = 1.665$ which can once again be found in the repository ($results/Anim\_u = 1,665 - 1S - Explicit.gif$). This plot also shows the period to be about π. This acts as a perfect example of the possible periodicity against quasiperiodicity of the system.

[3]Nick Tufillaro; Integrable motion of a swinging Atwood's machine. Am. J. Phys. 1 February 1986; 54 (2): 142–143. https://doi.org/10.1119/1.14710

[4]This is taken from the class notes

[5]Grazier, Kevin and Newman, William and Hyman, James and Sharp, P.W.. (2005). Long simulations of the Solar System: Brouwer's Law and Chaos. http://www.math.auckland.ac.nz/Research/Reports/view.php?id=527. 46. 10.21914/anziamj.v46i0.1008.

[6]Nicholas B. Tufillaro, Tyler A. Abbott, David J. Griffiths; Swinging Atwood's Machine. Am. J. Phys. 1 October 1984; 52 (10): 895–903. https://doi.org/10.1119/1.13791

By using μ and the period from the code above, we get Figure 3b which illustrates an improvement in the slope. Admittedly this is not by much but having a symplectic integrator would have made the improvement larger. This improvement is because in a periodic motion, over a full period where the update scheme is good, all the characteristics of the system should loop around thus giving the same state which and therefore the same energy.

An important case we had to consider when doing our integrator was the case of singular paths. Singular paths are paths that either start at r=0 or end there. In this paper we limit ourselves to the latter case. This singularity leads to division by 0 in our equations of motion which is a huge problem in both the motion and the energy of the system. To solve this problem, we simply end the simulation once the integrator reaches a specified threshold near r=0. While this means that in some cases the simulation might end early, in most cases our threshold of r = 10^{-1} was small enough to distinguish singular paths from non-singular ones.

5 Trajectories

As already stated, path can be divided in multiple categories. A good indicator of the performance of our integrator on non-integrable mass ratios μ is to compare the path for known quasiperiodic and non-singular μ with the path given by other integrators from literature. As we can see in Figure 4, we do indeed get quasiperiodic and non-singular paths with very small percentages in energy degeneracies.

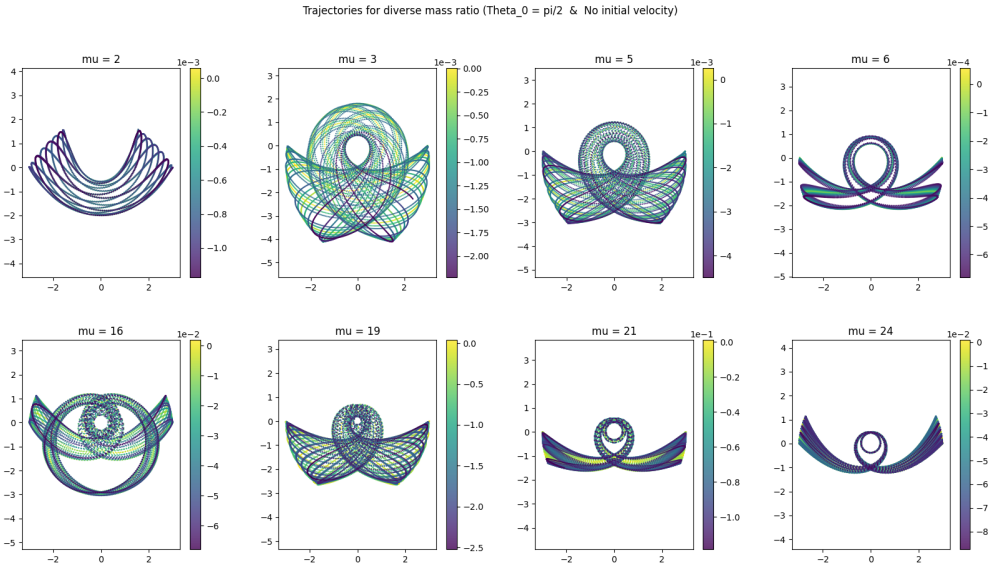

Figure 4: Quasi-Periodic trajectories colored by energy error (percentage)

These curves do indeed match visually with the numerical values and theoretical from the literature[7].

As such, since we do indeed get the characteristic we were researching, that the energy degeneracy is rather small and that the motion themselves map with what literature gives us, this is a strong argument that our integrator is indeed correct.

6 Lifetime of singular orbits as an indicator of instability

We have already studied some properties of non-singular paths and have quickly touched on how we handled singular one but the singular case has some interesting properties which can be uncovered. Such a trajectory can one again be viewed in the repository with $\mu = 10$ ($results/Anim\_u = 10 - 1S - Explicit.gif$).

One really interesting property of such motions is their lifetime. How does the lifetime of singular path evolve with respect to μ?

[7]Nicholas B. Tufillaro, Tyler A. Abbott, David J. Griffiths; Swinging Atwood's Machine. Am. J. Phys. 1 October 1984; 52 (10): 895–903. https://doi.org/10.1119/1.13791

One way to measure this is by doing simulations for a wide range of μ and collect their lifetime. We can do so like this:

```
...

tf = 500
dt = 0.01
maxU = 25
U = np.linspace(1.1,maxU+1,200)
x0 = np.array([ 3, 0, np.pi/2, 0 ])

DET = np.zeros(len(U))
t = np.zeros(len(U))

for i,u in enumerate(U):
    r,pr,theta,ptheta,dET = OneSwinging_2D_Explicit.integrate(u=u, tf=tf, dt=dt, x0=x0)
    DET[i] = max(abs(dET))
    t[i] = len(r)*dt
plt.plot(U,DET,label="Maximal Fractional Energy Loss")
plt.plot(U,5*t/max(t),label="5 * Fractional Time Length Of The Simulation")
...
```

The result can be seen in Figure 5 in which we also show the maximal energy error over the integration.
First, notice that the lifetime can be split into two categories: the μ which reach the final time and those who do not. The first category form the horizontal line and can be mapped to the non-singular motions while the second is the composed of the dips and the horizontal line at 0, these are the singular motions.
By comparing with the other results of this report, this binary categorisation does indeed lineup with all example used so far of non-singular motion, thus proving consistency.
One thing to note is that there is nearly no peaks near the top horizontal line which shows that the final time has been reached, this signify that all found singular path have lifetime significantly smaller the the total time over which we integrated, thus making our binary evaluation of singular or not accurate. Indeed, if we increase the final time, we will not see more singular point emerge.

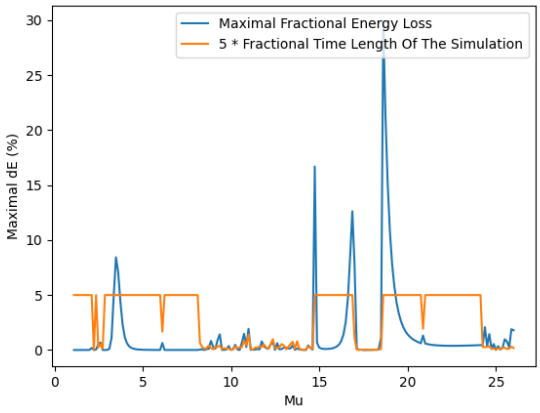

Figure 5: Energy Error and Lifetime by μ

The reason why we are also plotting the energy degeneracy is that it seems like there's a moderate correlation between the two. Indeed, for all singular points, we see that the the energy degeneracy seems to peak about the same points as the one where the life time is longer. By using numpy corrcoef after masking and normalization, we found a correlation coefficient of 0,46.

This correlation is expected since being close to the singularity obviously means a bigger error in energy.

We should also note that the very large peaks in energy near wells in lifetime are most likely due to the way we are handling the stop to our simulation when the system reaches singularity. Since the singular path go quickly within our threshold, and as such skip the portion near the singularity r=0, they also skip the zone where there is the most energy error. But on the other hand the non-singular paths around it go really close to it but do not end the simulation, thus leading to higher peaks than in the singular case. As such, a better singularity condition could be investigated to get better results.
Using more powerful computers to calculate a smaller dt could also be a good investigation since, according to our theory, the error should go really high in the well as the points near the singularity are now being resolved for those singular motion coming in with high velocity.

7 The two mass swinging case

First, we should preface by stating that this case is a lot more of a challenge. Indeed, no literature could be found about this specific system so no comparison to make sure our integrator was correct were available.
The system of two swinging masses extends the case with the single swinging mass by allowing the largest, second mass M, to also have angular momentum. Furthermore, we couldn't find any properly integrable μ to use as an analytical case. To integrate this system, we modified our integrator by applying the following changes on our implementation for the derivatives of the system:

```
...
def derivs(t,x):
    r,pr,theta_m,p_theta_m,theta_M,p_theta_M = x
    dr = pr/(M+m)
    dpr = -p_theta_M**2 / (M*(ropeLength-r)**3) + p_theta_m**2 / (m*r**3) -
        M*scipy.constants.g*np.cos(theta_M) + m*scipy.constants.g*np.cos(theta_m)
    dtheta_m = p_theta_m / (m*r**2)
    dp_theta_m = -m*scipy.constants.g*r*np.sin(theta_m)
    dtheta_M = p_theta_M / (M*(ropeLength-r)**2)
    dp_theta_M = -M*scipy.constants.g*(ropeLength-r)*np.sin(theta_M)

    return np.array([dr,dpr,dtheta_m,dp_theta_m,dtheta_M,dp_theta_M])
...
ET = pr**2 / (2*(M+m)) + ptheta_M**2 / (2*M*(ropeLength-r)**2) + ptheta_m**2 / (2*m*r**2) -
    M*scipy.constants.g*(ropeLength-r)*np.cos(theta_M) - m*scipy.constants.g*r*np.cos(theta_m)
...
```

The result of our new integrator can be seen in the repository ($results/Anim\_\mu = 3 - 2S - Explicit.gif$). As we can see, the energy error stays low enough for our case of $\mu = 3$.

Note that if we put the initial angle of mass M to be 0, we retrieve the case with one swinging mass as expected which is a good news.

We can once again plot the energy error after the entire integration time as a function of the number of step to compare with the known RK4 results. By doing so, we get Figure 6 where the slope and initial value are both near identical to the single swinging quasiperiodic case, which we already confirmed to be correct. As such, these results are just what we expect and we can say with confidence that, at least in the case where $\mu = 3$ which is used here, the energy of the distance is properly conserved given a large enough number of steps. Please note that we can only compare for what seems to be quasiperiodic over our time interval in this case as there are no known periodic μ to use when both mass are swinging.

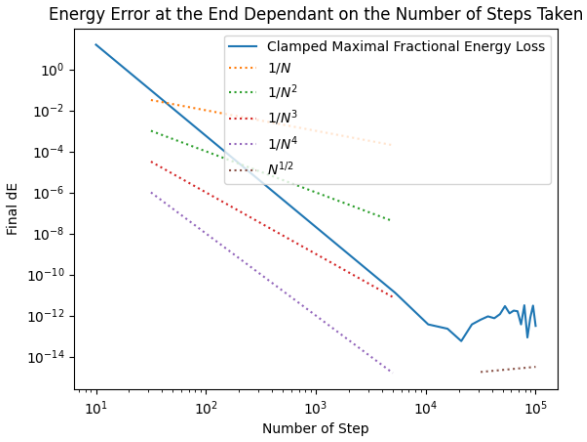

Figure 6: Energy Error by Number of step (μ=3)

We might as well create a plot of the trajectories of the mass m and M for the different μ we considered in Figure 4 so we can see the difference made by M having non-zero angular speed. By re-utilizing the same code with slight modifications, we can get Figure 7 for the mass m and Figure 8 for mass M.

An important takeaway of these trajectories is that they are not all quasiperiodic and non-singular like the one in Figure 4. As previously stated, the mass ratio $\mu = 3$ is still quasiperiodic with respect to the trajectory of the smaller mass m but this is not the case for mass M. Furthermore, we can see in the trajectories of mass M a somewhat repeating pattern for $\mu = 16$ and $\mu = 24$. Overall, the only real conclusions we can take from these figures are that the energy error seems to be pretty consistently small for different mass ratios μ and that the number of singular μ seems higher out of this small sample. These are things we will look into next.

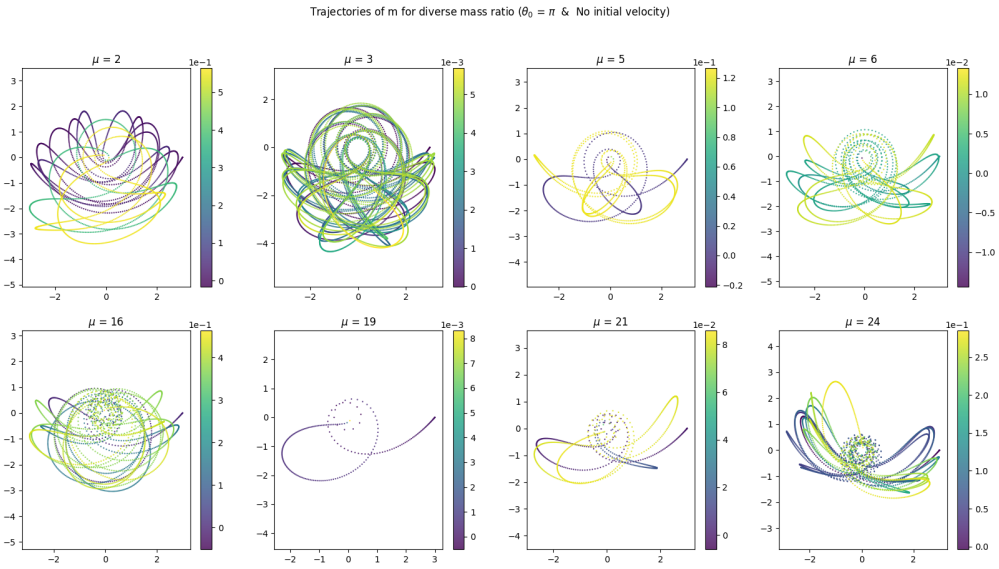

Figure 7: Trajectories colored by energy error of small mass m

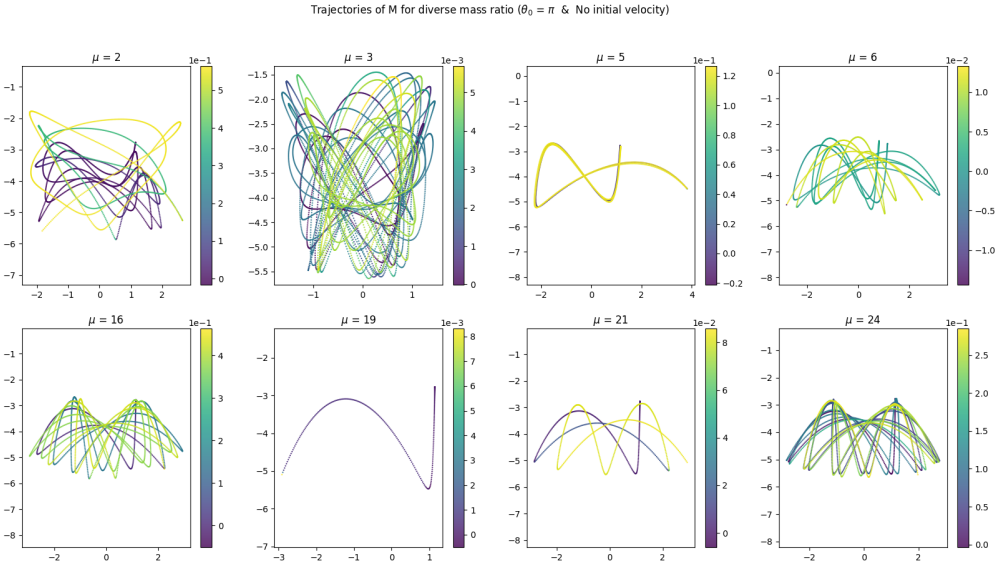

Figure 8: Trajectories colored by energy error of big mass M

In order to prove both of those assumption we will draw the same plot as Figure 5 but in our now two mass swinging system. By doing so we get Figure 9a for a final time of 100s and Figure 9a for a final time of 1000s. What we see here is very important because the plots in Figure 7 and Figure 8 were done with a time of 10s instead. The first noticeable thing in both plots is that the conclusions we did above are both true. The error is on average smaller than Figure 5 and we also see a lot more singular motions.
But, talking about the singular motion, we see by comparing the 100s case with the 1000s one that the case that were assumed to be quasiperiodic in the 10s are proven to be actually singular when increasing the final time which is contrary to what we concluded in Figure 5. This is a big conclusion for the system : there seems like all μ leads to singular motion. As such, we can say with confidence that the motion we assumed to be quasiperiodic non-singular for $\mu = 3$ in the analysis of Figure 6 was based on a wrong assumption as an increasing final time reveal the motion to

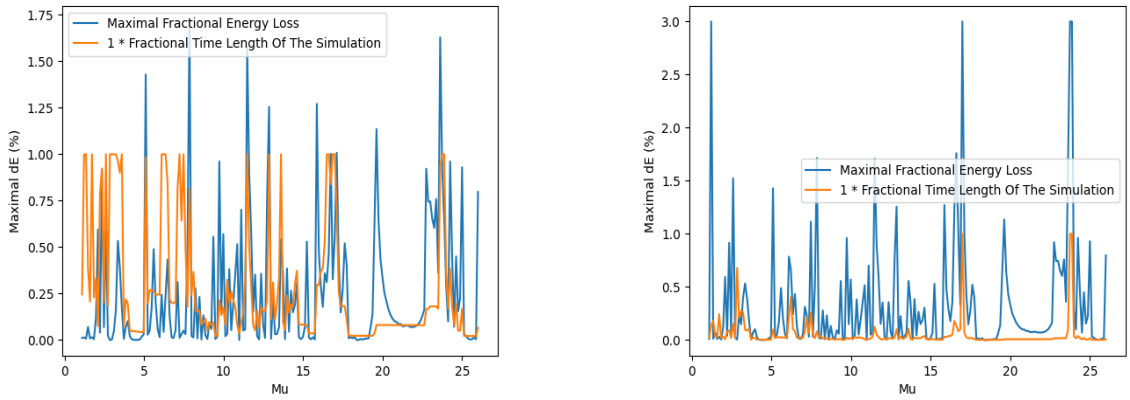

(a) Energy Error and Lifetime by μ with 2 swinging masses. $t_f = 100s$

(b) Energy Error and Lifetime by μ with 2 swinging masses. $t_f = 1000s$

Figure 9: Energy Errors and Lifetime by μ

actually be singular like all the other μ.

One last thing can be pulled out of these graphs. We concluded earlier for the one mass swinging case that there were a correlation between the energy error and the lifetime, lower lifetime (singular) would create zone of higher energy error around them. We can obviously cannot draw the same conclusion here since we have no plateau to draw those conclusions from. Although we seem to see a correlation between the sparse peaks in lifetime and peaks in error which could be explained as before for the edges of the plateau of the Figure5.

Overall, it is clear that the two swinging mass problem is way less instructive and nearly no clear conclusions can be drawn from it.

8 Future Improvement and Conclusion

9 Statement of Contribution